ELSEVIER

Polymer 41 (2000) 5053–5062

polymer

Structure–property relationships of void-free phenolic–epoxy matrix materials

C.S. Tyberg[a], K. Bergeron[a], M. Sankarapandian[a], P. Shih[a], A.C. Loos[a], D.A. Dillard[a], J.E. McGrath[a], J.S. Riffle[a,*], U. Sorathia[b]

[a]*NSF Science and Technology Center for High Performance Polymeric Adhesives and Composites, Virginia Polytechnic Institute and State University, Blacksburg, VA 24060, USA*

[b]*Naval Surface Warfare Center, 9500 MacArthur Blvd., West Bethesda, MD 20817, USA*

Received 25 January 1999; received in revised form 13 May 1999; accepted 18 May 1999

Abstract

The structure–property relationships of phenolic–epoxy networks have been investigated by several methods. Network densities have been explored by measuring the moduli in the rubbery regions and these experimental values were compared with those predicted from stoichiometry. The T_gs decreased, and toughness increased, as the phenolic Novolac content in the network was increased. Both results could be correlated to the decrease in network densities along this series. Analysis of the cooperativity of the networks suggests a crossover in properties from two competing factors, network density and intermolecular forces (hydrogen bonding). Measured fracture toughness values exceed those of typical untoughened epoxy networks and far exceed existing commercial phenolic networks. In addition, an increase in Novolac content improves the flame retardance rather dramatically. Thus, by controlling the Novolac content to reach an appropriate phenol to epoxy ratio, a void-free system with both favorable mechanical properties and flame retardance can be achieved.

Keywords: Phenolic; Epoxy; Flame retardance

1. Introduction

Phenolic resins, both Novolacs and Resols, are widely used commercially due to their excellent flame retardance and low cost [1–10]. There has also been significant interest in understanding the mechanisms of curing and decomposition of the phenolics in order to understand the reasons for their excellent flame retardance [2]. As a result of the low smoke generation of phenolic networks upon burning, they are the materials of choice in non-structural applications such as aircraft interiors [3]. Phenolics have a broad range of applications varying from construction to electronics and aerospace [11,12].

Commercial Novolac resins are normally cured with formaldehyde sources such as hexamethylenetetramine (HMTA) to form networks with relatively high crosslink densities [12,13]. Curing with HMTA however produces volatile by-products such as formaldehyde and ammonia, which lead to voids in the materials [14–20]. This has been a negative feature in forming phenolic matrix composites because the high void content results in brittle components. Therefore, current commercial Novolacs are limited to applications where high strength is not a requirement. On the contrary, epoxy resins are used for applications where high strength and toughness are needed, although they are highly flammable materials. The flame retardance of epoxy resins can be improved by incorporating bromine into the structure, but bromine also increases toxic smoke emission [21].

Phenolics have been used as curing agents for epoxy resins where the epoxy is usually the major component [22,23]. In many cases, these systems make up the base resins for semiconductor packaging due to their improved hydrophobicity relative to amine-cured epoxies and their low cost. Effects of crosslink densities on the physical properties of the networks have been studied [24]. Unfortunately, these systems do not have good flame resistance because of the high content of flammable epoxy resin.

This paper focuses on curing phenolic resins with epoxies as opposed to HMTA (Fig. 1) [25]. Network density can be at least somewhat controlled by the stoichiometric offset between phenol and epoxy groups. The approach is to utilize networks high in phenolic content (up to ~80 wt%) so that

* Corresponding author. Tel.: +1-540-231-8214; fax: +1-540-231-8517.
E-mail address: jriffle@aol.com (J.S. Riffle).

0032-3861/00/$ - see front matter
PII: S0032-3861(99)00574-1

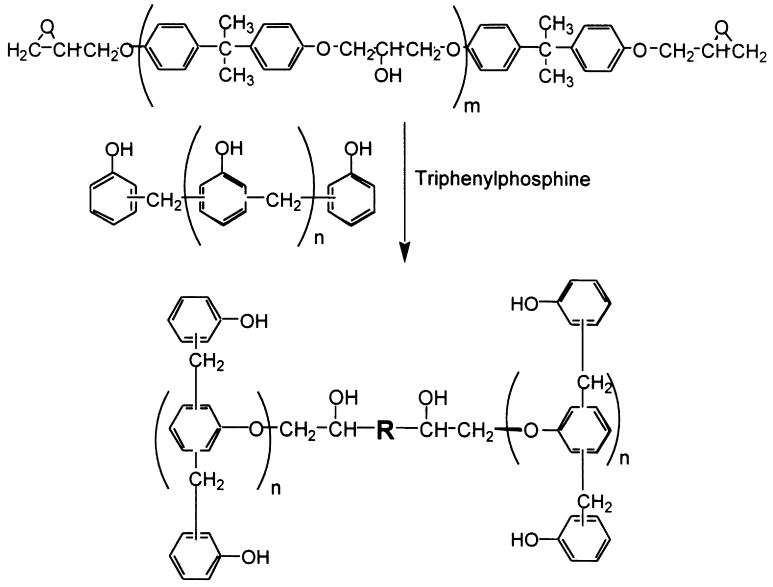

Fig. 1. Network formation of phenolic Novolacs cured with epoxies.

the fire retardant properties of the phenolic material are retained while tailoring mechanical properties via crosslink densities and molecular structure. In addition, these systems are tougher than the phenolic Novolac resins cured with HMTA as a result of the lack of voids in the networks. The intent is to prepare materials as strong as epoxy networks, which retain the flame retardance of phenolics [26,27]. This work focuses on the structure–property relationships with different compositions of phenolic and epoxy oligomers.

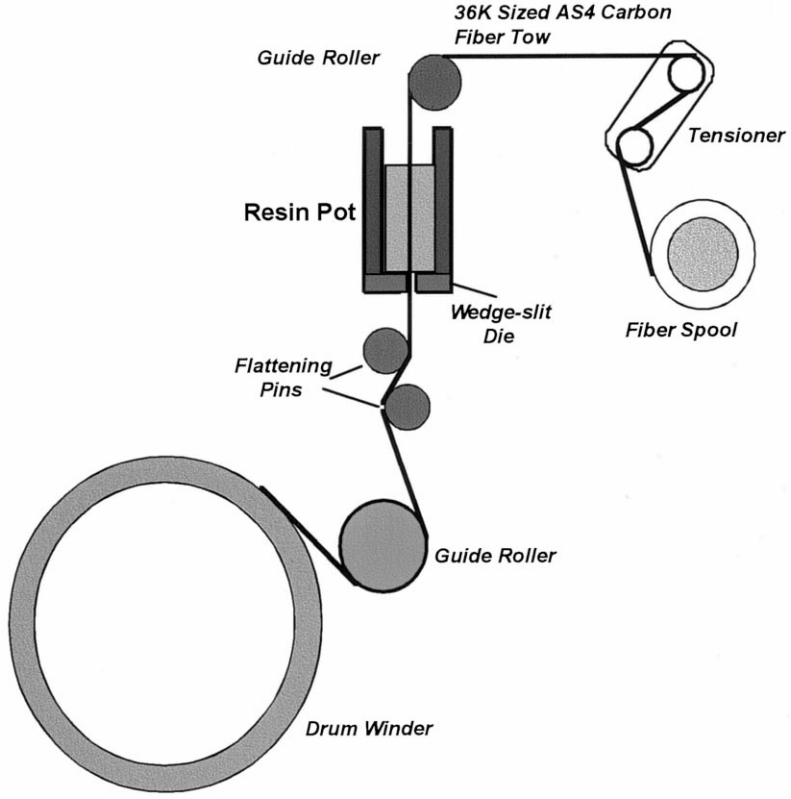

Fig. 2. The hot-melt prepregging process.

2. Experimental section

2.1. Materials

The commercial phenolic resins were kindly provided by Georgia-Pacific (Product #GP-2073). The phenolic resin used had a number average molecular weight of ~741 g/mol. Epon 828 epoxy resin was obtained from Shell Chemical. Triphenylphosphine (TPP) was obtained from Aldrich and used as received. AS4 35 K carbon fiber tow was obtained from Hexcel. E-Glass fabric (style 162) was obtained from Clark-Schwebel (now Hexcel).

2.2. Network preparation

To a three neck round bottom flask equipped with a vacuum tight mechanical stirrer and a vacuum adapter was added phenolic Novolac and ~75% (by wt.) of the required epoxy. The flask was heated in an oil bath to 170°C. When the Novolac began to soften at 170°C, mechanical stirring was begun. Vacuum was applied incrementally to prevent the material from swelling into the vacuum line. Once full vacuum was achieved (2–5 Torr) the solution was stirred for about 20 min to degas the blend. During this time the remaining epoxy, with the TPP catalyst (0.1 wt% based on the total weight of epoxy) dissolved in it, was degassed in a vacuum oven at ~80°C. The stirring solution was cooled to 140°C, and the vacuum was temporarily released to add the remaining epoxy with catalyst. This was stirred for about 4 min to fully degas the samples. The melt was then poured into a mold (which had been preheated to 180°C) in a preheated oven and covered with mold release cloth and a heavy metal plate. The samples were cured at 180°C for 1 h and then 200°C for 1 h. The cure schedules were established using isothermal differential scanning calorimetry (DSC) measurements of heats of reaction to determine appropriate conditions for full cure, as well as dynamic mechanical analyses (DMA) to determine T_gs of the cured samples. The samples cured by the indicated cure cycles showed no change in T_g with additional heating, indicating that the samples were fully cured. Prior to mechanical testing all samples were heated to 180°C for 45 min, then cooled slowly in the oven to room temperature. This was done to give all samples the same thermal history.

2.3. Hot-melt prepregging and composite fabrication

A lab scale Model 30 prepregger manufactured by Research Tools Corporation, Ovid, Michigan was used in composite preparation (Fig. 2). In this apparatus, a 36K sized AS4 carbon fiber tow was passed through a wedge-slit die at the bottom of a heated resin pot containing the matrix resin. The wetted tow was then passed between a pair of flattening pins and around a guide roller before being wound on a drum. The flattening pins and the guide rollers were independently heated. Unidirectional carbon fiber prepregs were prepared with various uncatalyzed phenolic/epoxy resin compositions using the hot-melt technique. The set-point temperatures of the resin pot, flattening pin, and roller, were determined by viscosity data. The set-point temperature was 120°C for the 50/50 (wt/wt) phenolic/epoxy and 140°C for the 70/30 (wt/wt) and 80/20 (wt/wt) phenolic/epoxy resins. These high temperatures were necessary to give a low enough melt viscosity to process the materials. Low melt viscosities of the resins are critical to permit good wet-out of the reinforcing fiber tows and yield uniform resin content. The prepregs are then cut and placed in a metal mold and cured with a thermal cycle of 230°C for 4 h to make composite panels. This cure cycle was determined by DMA to give the highest T_g, comparable to that of the catalyzed materials, indicating that it is sufficient to promote complete cure of the uncatalyzed systems. The weight fraction of fibers in the composites was 74–77% fiber for the glass fabric and 74–79% fiber for the carbon fiber. The fiber weight fraction of the glass fabric composites was determined by dividing the weight of the fabric by the weight of the composite. The glass fabric had 28 yarns/in. in the warp direction, and 16 yarns/in. in the weft direction. The panels for mechanical testing were 12 ply and $6'' \times 6''$. The fiber weight fraction of the carbon fiber composites was calculated from the measured composite densities and the densities of the fiber and cured neat networks.

2.4. Measurements

DSC measurements were carried out using a Perkin–Elmer differential scanning calorimeter, model DSC-7. Samples of about 8–12 mg were placed in aluminum pans and cured using a dynamic temperature scan from 30 to 260°C with a heating rate of 5°C/min. The peaks in the reaction exotherms were used to determine network cure temperatures and rates. Activation energies were obtained following ASTM E 698, with a correction for the influence of heating rate on temperature. The correction was calculated by the deviation in the melting point of indium from the accepted value of 156.60°C.

Relaxation tests to determine storage modulus versus time were performed using a Dynastat calibrated using digital calipers accurate to 0.01 mm. The Dynastat was designed for materials testing: performing creep, relaxation, and dynamic tests. The oven temperature is controlled automatically, with a range of −150 to 250°C.

The test specimens, with dimensions of height b (3.18 mm), width w (6.35 mm), and length l (38.1 mm), were placed on two flat supports with a span of 2.54 cm, in the three-point bend setup. Samples were heated to 70°C below their T_g (determined from the peak in the tan delta curve obtained by DMA). At this temperature, a constant displacement of 0.1 mm was applied to the sample (0.1 mm displacement was reached in less than 1 s). The load was recorded over a period of 1000 s. At this point the displacement was removed and the sample was allowed to recover

Table 1
Physical properties of phenolic/epoxy networks

Phenolic/epoxy (wt/wt)	Phenolic/epoxy (eq/eq)	ρ (25°C)	ρ (T_g + 60°C)	T_g (°C)	Modulus at T_g + 60°C (Pa)	M_c (measured)	M_c (theoretical)
50/50	1.8/1	1.215	1.162	151	2.09×107	644	492
65/35	3.3/1	1.230	1.178	127	9.35×106	1413	3564
80/20	7.2/1	1.240	1.167	114	2.87×106	4539	∞

for 2000 s (~35 min). The temperature was then increased by 5°C and the cycle was repeated until the temperature had reached 35°C above the T_g. The displacement at each temperature increment was slightly greater due to the thermal expansion of the sample and the instrument. The thermal expansion of both the instrument and sample were used to calculate the corrected displacement (instrument expansion is 0.0033 mm/°C, sample is ~0.0005 mm/°C in the glassy state and ~0.00015 mm/°C in the rubbery state). The moduli were calculated from the measured load and displacement values by Eq. (1)

$$E = g(P\Delta)(L^3/48\mathrm{I}) \quad (1)$$

P/Δ is the slope of load versus displacement data, g the gravitational constant is 9.81 m/s^2, L the length between the supports is 2.54 cm and I is $(1/12)wb^3$.

Creep tests, using a Dynastat, were performed to determine the rubbery moduli at 60°C above the glass transition temperatures. The samples were heated to 60°C above T_g, a small load (0.01 kg) was placed on the samples and the displacements at equilibrium were measured. Equilibrium was obtained in less than 3 s, indicating that the material was in the rubbery plateau region at the testing temperature of T_g + 60°C. The load was increased by increments of 0.01 kg up to about 0.08 kg and at each load the equilibrium displacement was recorded. From this data, load versus displacement curves, were generated and linear regression analyses were used to determine the slopes of the lines. These slopes were used to determine the moduli according to Eq. (1). The displacement values measured from the Dynastat are accurate to within 0.05 mm.

Room temperature density measurements were conducted using a Mettler-Toledo AG204 balance adapted with a Mettler-Toledo density determination kit for AT/AG and PG/PR balances. Rectangular samples with dimensions of approximately $19 \times 6.35 \times 3.18$ mm were sanded, then polished, to prevent any trapping of air bubbles. Deionized water was degassed in the vacuum oven at 23°C for about 30 min prior to use. Using this setup, the weight of the solid in air (A) and the weight of the solid in water (B) were measured. The temperature of the water was recorded to within 0.1°C and the density of distilled water at that temperature was obtained from a density table. Room temperature densities were calculated according to Eq. (2) (Table 1)

$$\rho = \{A/(A - B)\}\rho(\mathrm{H_2O}) \quad (2)$$

The densities at 60°C above T_g were calculated using the coefficients of thermal expansion below T_g and above T_g, measured by thermal mechanical analysis using the large quartz parallel plate measuring system in TMA mode. Using these densities and the rubbery elastic moduli (determined from Dynastat measurements) the molecular weights between crosslinks (M_c) were calculated by Eq. (3)

$$M_c = 3\mathrm{R}T\rho/E \quad (3)$$

DMA were used to determine the glass transition temperatures. These measurements were performed using a Perkin–Elmer dynamic mechanical analyzer, model DMA-7. The T_gs were calculated from the peaks in the tan delta curves. The analyses were conducted using a three-point bend set-up with rectangular specimens. The tests were run with tension control set at 110% using amplitude control adjusted to set the room temperature modulus to 1×10^9 Pa. Fully cured samples were heated at 5°C/min from 25 to 200°C.

Three-point bend tests were utilized to characterize the toughness of the phenolic–epoxy networks in terms of the critical stress intensity factor K_{1c}, according to ASTM standard D 5045-91 [28]. The specimens had thickness b (3.12 mm) and widths w (6.28 mm). The single edge notch bending method was used. First, a sharp notch was created in the sample by sawing. A natural crack was initiated by inserting a cold razor blade (which had been immersed in liquid nitrogen) into the notch and tapping with a rubber hammer. The depth of the crack (a) was between 40 and 60% of the width (w). The pre-cracked notched specimen was loaded crack down, into a three-point bend fixture and tested using an Instron model 4204 instrument. The single edged notched bending rig had moving rollers to avoid excess plastic indentation. The three-point bend fixture was set up so that the line of action of applied load passed midway between the support roll centers within 1% of the distance between these centers. The crosshead speed was 1.27 mm/min, and the testing was conducted at room temperature.

Flame retardance was directly measured using cone calorimetry on void free neat panels (no fiber), as well as carbon and glass fiber composites, in a horizontal orientation. Panels with a surface area of ~0.01 m^2 and 6.35 mm thick were used with an incident radiant heat flux of 50.0 kW/m^2 for the neat resins, and 75 kW/m^2 for the composite panels.

Soxhlet extractions with methyl ethyl ketone (MEK) were used to determine the sol fractions of the networks. Cellulose thimbles were soaked in MEK for 24 h then dried

in the vacuum oven at room temperature for 24 h. They were subsequently heated to 140°C for about 12 h. After the samples were allowed to cool to room temperature in the vacuum oven, they were weighed within 30 s of releasing the vacuum and the weight was recorded. Samples were extracted for 72 h, placed in the vacuum oven at room temperature for 24 h, then heated to 140°C under vacuum for about 12 h and allowed to cool to room temperature under vacuum. After being removed from the vacuum oven, the thimbles containing the samples were weighed within 30 s to prevent any significant weight gain due to moisture absorption.

2.5. Composite panel characterization

The composite panels were C-scanned for overall quality using a sonix model HF 1000 instrument by a pulse–echo arrangement using a 15 MHz transducer with a focal length of 38.1 mm. Scanning electron photomicrographs, obtained from an ISI SX-40 SEM, were used to establish the void free nature of the composites and to confirm good resin distribution and fiber wet-out. Transverse and longitudinal flexural tests following ASTM standard D-790 were used to evaluate a systematically varied series of phenolic/epoxy compositions.

3. Results and discussion

A phenolic Novolac resin with an average functionality of 7.3 phenolic groups was cured with a bisphenol-A based epoxy with an epoxy equivalent weight of 187 g/mol. Systematically varied compositions were studied ranging from 50 to 80 wt% phenolic Novolac. Structural and compositional effects on cooperativity, network toughness, transition temperatures, and flame retardance were evaluated.

In general, network toughness would be expected to increase with the average molecular weight between crosslinks (increase in ratio of phenols to epoxies) up to some point where the amount of unconnected phenolic chains begins to dominate properties. Likewise, glass transition temperatures of fully cured networks should decrease as the distance between crosslinks increases. Thus, it was of interest to predict and measure network densities and correlate these chemical structures to physical properties of the networks. “Theoretical” average distances between crosslinks were predicted by considering the stoichiometries and assuming a linear phenolic chain (Table 1). In considering the chemical structures of these networks, it was predicted that the crosslink densities should decrease as the stoichiometric offset (excess of phenols) was increased. These predicted values were then compared to experimental measurements of crosslink densities derived from rubbery moduli and elasticity theories.

The following assumptions were made in order to predict the molecular weights between crosslinks: (1) all chains were of equal length (any effects of molecular weight distributions were not considered); (2) a segment was defined by any chain connected by two junction points; and (3) a junction point was defined as a point were at least three segments intersected. The number of segments for each system was calculated based on the stoichiometric ratio of epoxy to phenol and the average functionality of the phenolic chains ($f = 7.31$). The calculation for M_cs involves dividing the total molecular weights of all chains considered by the total number of segments. This method should correlate well to measured values for cases where very few “dangling ends” (i.e. elastically inactive segments) exist. The number of so-called dangling ends would be minimized when the phenolic chains were either very long or for cases where the crosslink density was very high. On the contrary, since this method for calculating M_c includes the total weights of all the chains considered (including the weights of the dangling ends) and it does not count those chain ends as segments, then the theoretical values should be higher than those calculated from rubbery moduli data.

According to rubber elasticity theory, the rubbery moduli of these networks should be proportional to the crosslink densities. Absolute values for the moduli in the rubbery plateau regions were determined from creep tests at 60°C above T_g using a Dynastat. The slopes of the load versus displacement curves were used to calculate moduli according to Eq. (1), then the molecular weights between crosslinks (Table 1) were calculated (Eq. (3)) from the moduli and densities at 60°C above T_g. Eq. (3) was derived to apply to elastically active network chains only (not dangling ends or unconnected chains). Therefore, the networks with the highest number of dangling ends would be expected to deviate most significantly from the theoretical predictions [30]. The experimental trend in M_c follows the expected increases with stoichiometric offset (higher ratios of phenols to epoxy groups) in all cases. The experimental M_c values, however, are lower than those predicted from stoichiometry for the materials with the lower network densities (Table 1). This difference can probably be attributed to the large distribution of molecular weights of the phenolic oligomers, which was not considered in the theoretical predictions, and the fact that as the ratio of phenols to epoxies is increased, the number of chains which do not contribute to networking increase (i.e. the number of dangling ends increases).

For the system under study, it should be noted that crosslink density is not the only factor affecting the physical properties of the networks. As the compositions were varied from 2/1 to 7/1 phenol–epoxy equivalence ratios, the network densities decrease, but at the same time the glassy intermolecular forces increase along this series, due to an increase in hydrogen bonding from the larger numbers of unreacted phenols. Therefore, the composition with the lowest network density has the highest amount of unreacted phenols, and highest hydrogen bonding capability. This causes the glassy moduli of the materials having the lower network densities to be unusually high. This is illustrated in

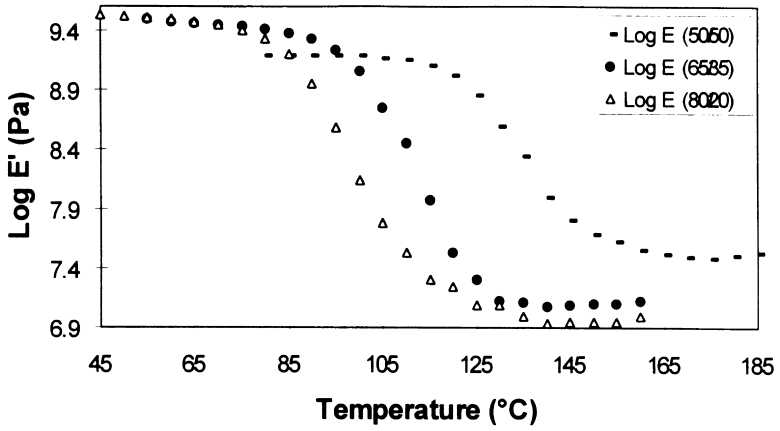

Fig. 3. Ten-second storage modulus vs. temperature.

the 10 s storage moduli versus temperature curves which were generated from the relaxation data for each composition (Fig. 3). It is evident from these curves that the rubbery moduli follow the trends expected based on crosslink densities, e.g. as crosslink density decreases the rubbery modulus decreases. On the contrary, the glassy moduli seem to run in the opposite direction. These results can be further understood using a cooperativity analysis, which will be discussed in the following paragraphs.

Influences of network structure on the physical properties was further probed by analyzing relaxation moduli. Relaxation modulus versus time curves were generated at 5°C temperature increments from the glassy to the rubbery regions. From these curves, a master curve was generated for each composition based on the time–temperature superposition principle, with no vertical shifting (Fig. 4). The shift factors (log a_T) used in generating the master curves were plotted as a function of the temperature ($T - T_g$). Both the master curve and the shift factor plots were uniform indicating that the time–temperature superposition principle

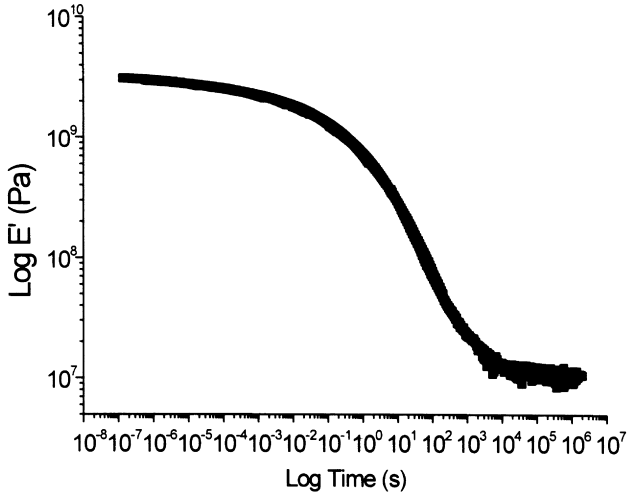

Fig. 4. Examplary modulus vs. time master curve (65/35 phenolic/epoxy).

was valid for these networks. Graphs of the shift factors (log a_T) as a function of the T_g normalized temperature (T_g/T) were generated for three compositions (Fig. 5). The indicated range is limited in temperature resulting in the linear appearance of the curves. Slopes of the curves in the linear region, at $T = T_g$, were determined from linear regression of the data (Table 2). These provide a measure of the fragility (m) of the networks (Eq. (4)). The WLF equation did not show a good fit to the data at higher temperatures and therefore was not used in any calculations for cooperativity

$$m = [\mathrm{d}\log(a_T)/\mathrm{d}(T_g/T)] \qquad \text{at } T = T_g \tag{4}$$

The fragility, m, describes the increase in the most probable segmental relaxation time with a decrease in temperature, in close proximity to the glass transition region. Therefore, a large m implies that the rate at which the degree of cooperativity changes with decreasing temperature is higher. This has been previously correlated to an increase in crosslink density [29]. Likewise, an increase in fragility (m) has also been associated with an increase in potential for secondary bonding [30–32]. In this phenolic/epoxy network series, the expected direction of m is interesting (but difficult to predict) due to the two competing effects, crosslink density and hydrogen bonding. Based on the molecular weights between crosslinks one might expect a decrease in m as the offset in stoichiometry is increased from 1.8/1 to 7.2/1. This is not what has been observed, there seems to be a maximum in the fragility instead of a linear trend, with the 3.3/1 network having the highest m value. The fragility calculated from the T_g normalized Arrhenius plot at $T = T_g$, suggests that both the crosslink density and hydrogen bonding are important factors affecting the glass formation processes for these networks (Table 2). The fact that there appears to be a maximum in the cooperativity at the middle composition (3.3/1) suggests a crossover of the two competing factors, network density and hydrogen bonding.

In addition, the master curves were fit with the KWW equation (Eq. (5)) to solve for the β parameters for each composition (Table 2). These β parameters have been

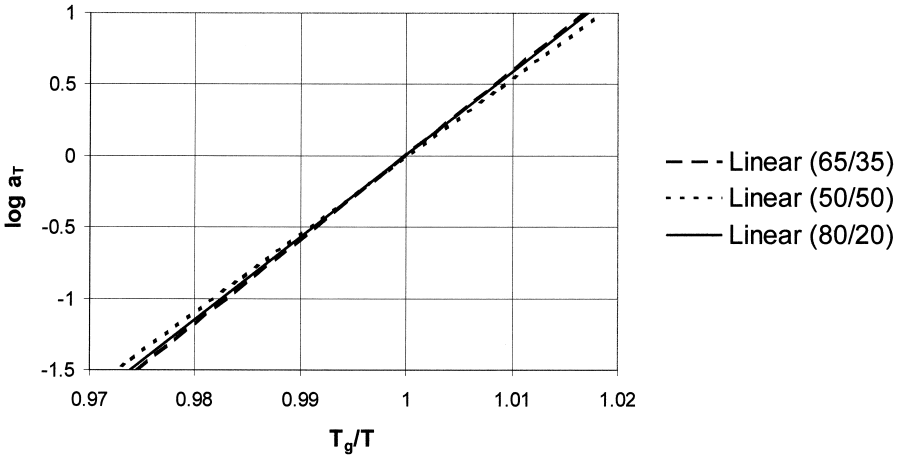

Fig. 5. Fragility plot to detemine *m*.

shown to have some correlation with fragility, *m*, for many glass forming materials, although the two have different physical meanings and are derived from different concepts [33]. The KWW parameter β is a measure of the breadth of the distribution of segmental relaxation times. Therefore a smaller value for β suggests a broader distribution of relaxation times, which relates to a more cooperative system [34]. It has been shown previously that a decrease in M_c correlates with a lower β and therefore a broader relaxation response [34]. Just as with the fragility measurements, the data for these phenolic/epoxy networks does not follow this trend, probably as a result of the higher intermolecular forces for the systems with the lower network density. There is a minimum in β for the 3.3/1 composition indicating that this composition is the most cooperative network.

For the phenolic/epoxy networks under study, there is good correlation between *m* and the KWW exponent β (Fig. 6). The decreasing trend in *m* as β increases is consistent with the trends found by Bohmer et al. [33]. Therefore the interpretation of relaxation response using the relaxation time breadth parameter (β) suggests a consistent measure of cooperativity in comparison to that determined by the fragility approach

$$\phi(t) = \exp[-(t/\tau)]^{\beta} \quad (5)$$

Dynamic mechanical analysis was used to determine the glass transition temperature of each composition. The T_gs were calculated from the peaks in the tan delta curves (Table 1). The results of these DMA analyses show that as the stoichiometric offset (excess of phenols) was increased, the T_gs of the networks decreased. This was the expected trend due to the expected decrease in network density in going from 2/1 (phenol/epoxy) to 7/1 (phenol/epoxy).

Network fracture toughness was determined by measuring the plane-strain stress intensity factors, K_{1c}. Higher values of K_{1c} indicate improved resistance to crack propagation, i.e. increased toughness. Toughness increased with the increased offset in stoichiometry to a maximum of 0.85 MPa-m$^{3/2}$ for the 3/1 phenol/epoxy networks (Table 3). This is consistent with the drop in moduli and decrease in network density. The toughness decreases slightly when the stoichiometric offset becomes too large (7/1 phenol/epoxy). This is undoubtedly related to the increase in dangling ends and unconnected phenolic chains at these very high phenol-to-epoxy ratios. Most of the materials with a phenolic Novolac content of 50 wt% or greater have significantly higher toughness than the epoxy control (bisphenol-A based epoxy stoichiometrically cured with *p*,*p*′-diaminodiphenylsulfone). This is considered a breakthrough because the commercially cured phenolic resins are much more brittle than epoxies. Thus, it can be reasoned that phenolic–epoxy mechanical properties using this particular phenolic oligomer can be optimized by controlling stoichiometry at approximately 3/1 phenol to epoxy. Lower ratios lead to increased brittleness associated with higher network densities, and higher ratios result in too many dangling ends and unconnected chains for optimum

Table 2
Cooperativity parameters

Phenolic/epoxy (wt/wt)	Phenolic/epoxy (eq/eq)	M_c (measured)	Cooperativity(m) $d(\log a_T)/d(T_g/T)T = T_g$	β((KWW fit)
50/50	1.8/1	644	54.8	0.258
65/35	3.3/1	1413	59.2	0.203
80/20	7.2/1	4539	57.7	0.218

Table 3
Sol fraction and fracture toughness of phenolic/epoxy networks

Phenolic/epoxy (eq/eq)	Phenolic/epoxy (wt/wt)	Sol fraction	K_{1c} (MPa $m^{1/2}$)
Control (epoxy 1 cured w/DDS)	–	–	0.62
1/1	36/64	2.6	0.57
2/1	53/47	3.4	0.64
3/1	63/37	12.5	0.85
7/1	80/20	24.5	0.70

Table 4
Flame retardance of phenolic/epoxy networks

Phenolic/epoxy (wt/wt)	Peak heat release rate (kW/m^2)	Char yield (wt%)	Smoke toxicity (CO yield/CO_2 yield) ($\times 10^{-3}$)
Control epoxy (epoxy/DDS)	1230	5	44
35/65	477	17	45
50/50	382	23	36
65/35	357	29	34
80/20	260	33	27

mechanical properties. It is interesting to note that the ratio that shows the highest toughness also has the highest degree of cooperativity, as determined from the m and β parameters.

The flame retardance of neat panels of the phenolic/epoxy networks was measured using a cone calorimeter with a heat flux of 50 kW/m^2 and 20.9% O_2 (atmospheric oxygen). The heat release rate curves from the phenolic/epoxy networks show a much lower peak heat release rate and lower total heat released than the epoxy control. The heat release rate of the 80/20 (wt/wt) phenolic/epoxy network never reaches 300 kW/m^2; whereas the epoxy control has a maximum heat release rate of about 1200 kW/m^2 (Table 4). From the cone calorimetry data we know that the networks have a high degree of flame retardance, but we do not fully understand what the factors involved in the flame retardance are. One possibility is that the free phenolic groups on the Novolac may act as free radical traps to retard degradation at the burning front. It was reasoned that such behavior might result in the feed of volatiles to the flame being reduced. Another possibility is that the high aromatic content of the phenolic resin leads to a high char yield at the burning surface. The char would not burn readily, and might also shield heat conduction from the flame to the substrate. High char yields for the networks high in phenolic content were observed by cone calorimetry (Table 4). These thermograms show that materials with a higher content of phenolic material in the network have higher char yields.

3.1. Composite properties

Scanning electron microscopy (SEM) was used to

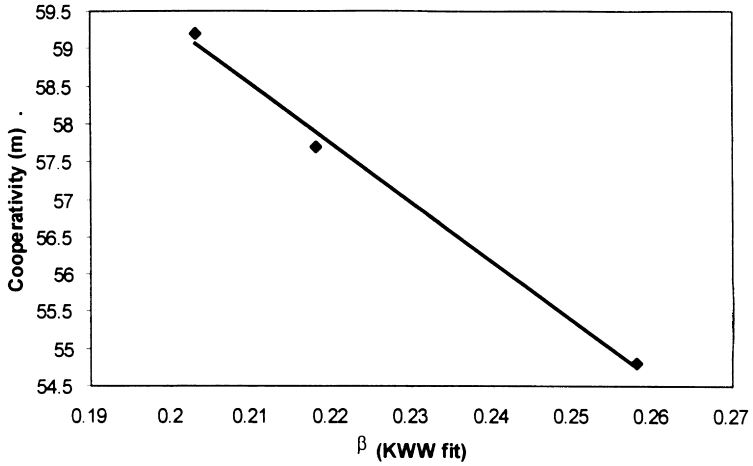

Fig. 6. Correlation between fragility, m, and the KWW parameter β.

Table 5
Transverse and longitudinal flexural strengths and moduli of carbon fiber reinforced composites

Novolac/epoxy (wt/wt)	0° Flexural strength (MPa)	90° Flexural strength (MPa)	0° Flexural modulus (GPa)	90° Flexural modulus (GPa)
Control epoxy (epoxy 1/DDS)	1389	29	159	8.9
50/50	2051	63	156	12.1
70/30	2020	66	162	11.3
80/20	1808	39	174	11.1

Table 6
Flexural strengths of glass fabric reinforced composites

Novolac/epoxy (wt/wt)	Warp flexural strength (MPa) (28 strands/in.)	Weft flexural strength (MPa) (16 strands/in.)
Control epoxy (epoxy/DDS)	442	367
50/50	436	351
70/30	567	372
80/20	379	261

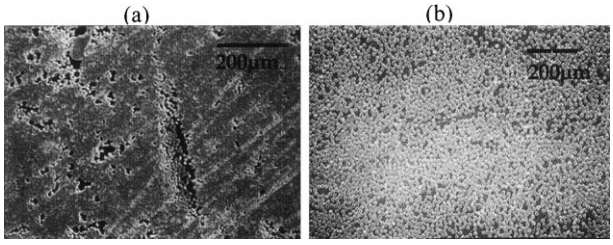

Fig. 7. SEM Micrographs of unidirectional carbon fiber reinforced composite cross-sections: (a) commercial phenolic resole matrix; and (b) phenolic/epoxy networks

confirm the void-free nature of the composites. Images of composite cross-sections prepared with a commercial phenolic matrix (from a resole resin), and one of the phenolic/epoxy matrices described herein is depicted in Fig. 7. It is evident that the void content is greatly reduced in the phenolic/epoxy system. No voids are evident in the representative region scanned.

Unidirectional carbon fiber reinforced composites made with the phenolic/epoxy resins exhibited superior transverse and longitudinal flexural strengths and moduli compared to the epoxy control (Table 5). The panels prepared from the 50/50 and 70/30 (wt/wt) phenolic/epoxy compositions exhibited the highest values, consistent with the superior toughness of these materials, which were measured for the neat networks. The excellent transverse flexural properties of the phenolic/epoxy compositions may also reflect improved fiber/matrix adhesion. This might be expected due to the unusually high potential for hydrogen bonding inherent in the chemical backbone structure for the phenolic material. Glass fabric reinforced composites prepared from the 70/30 (wt/wt) phenolic/epoxy resin exhibited superior warp and weft flexural strength, exceeding the epoxy control as well as the other phenolic/epoxy ratios (Table 6). This is also consistent with the fracture toughness of the neat networks.

Cone calorimetry measurements were performed on carbon and glass fiber composites of both the epoxy control, and the 80/20 (wt/wt) phenolic/epoxy network. The weight percent matrix in the composites, were 24% for the carbon and 25% for the glass. This is important, in that, only about 20% of the total weight was lost in the flammability experiments with an incident heat flux of 75 kW/m^2. This results in a smaller change in properties between samples as compared to the analogous data on neat networks. In spite of this, as expected, both the carbon and glass fiber composites with the phenolic/epoxy system show reduced heat release rates, mass loss rates, and specific extinction areas relative to the epoxy controls (Table 7).

4. Conclusions

Relationships between the chemical network structures and the physical and flame performance properties of new phenolic–epoxy materials have been elucidated. Network densities have been explored by measuring the moduli in

Table 7
Composite flame retardance

Property	Phenolic/epoxy (carbon)	Epoxy control (carbon)	Phenolic/epoxy (glass)	Epoxy control (glass)
% Consumed	19.2	22.9	15.9	21.7
Avg. HRR (kW/m^2)	72	105	81	93
Total heat released (MJ/m^2)	38.7	57.5	44.8	54.8
CO/CO$_2$	0.0262	0.0378	0	0
Avg. mass loss rate (g/s m^2)	4.2	9.0	6.6	9.0
Avg. SEA (m^2/kg) (specific extinction area)	672	1060	874	1052

the rubbery regions and these experimental values were compared with those predicted from stoichiometry. At least trends in experimental results followed predictions. The T_gs decreased, and toughness increased, as the phenolic Novolac content in the network was increased. Both results could be correlated to the decrease in network densities along this series. Cooperativity studies suggest correlation between the parameters m and β, and suggest a crossover in properties from the two competing factors, network density and intermolecular forces. Toughness values exceed those of typical untoughened epoxy networks. In addition, an increase in Novolac content improves the flame retardance rather dramatically. The maximum flame retardance was achieved for networks with 80 wt% of the phenolic component, and these networks have significantly better flame retardance than the epoxy control. Thus, by increasing the Novolac content to reach a phenol to epoxy ratio of about 3/1, the combination of mechanical properties and flame retardance is improved simultaneously.

5. Future work

One aspect of future research in this area will be focused on increasing the processing window of the phenolic/epoxy systems for rapid "on-line" composite fabrication techniques such as pultrusion or resin infusion. Other directions for pursuit will be in identifying epoxy components containing silicon and phosphorus in order to improve flame properties even further.

Acknowledgements

The authors are grateful for the financial support of the NSF Science and Technology Center for High Performance Polymeric Adhesives and Composites at Virginia Tech (DMR 9120004) and to the GenCorp Foundation. They are also grateful to the Dow Chemical Co., Shell Chemicals and to Georgia-Pacific Corp. for materials donations and for close technical cooperation. The authors are also grateful to Dr C. Robertson for technical discussions.

References

[1] Hshieh F, Beeson HD. Fire and Materials 1997;21:41–49.
[2] Antony R, Pillai CKS. J Appl Polym Sci 1994;54:429–438.
[3] Kunz HE. Macro Chem, Macromolecular Symposium 1993;74:155–164.
[4] Dailey Jr TH. Plastics Engng 1989;33–36.
[5] Sorathia U, Lyon R, Ohlemiller T, Grenier A. Review of fire test methods and criteria for composites. SAMPE Journal 1997;33(4):23–31.
[6] Scudamore MJ. Fire performance studies on glass-reinforced plastic laminates. Fire and Materials 1994;18(5):313–325.
[7] Elmer C, Mestdagh JJ. Monsanto Co. US Patent 3,352,744. Self-Extinguishing Phenolic Resin Compositions and Laminates Prepared Therefrom. 11/14/67.
[8] Schwarzer CG. Shell Oil Co. US Patent 3,369, 056. Flame Retardant Phenolic Resin Compositions. 2/13/65.
[9] Fire and Smoke Resistant Interior Materials for Commercial Transport Aircraft. NMAB -477-1. National Materials Advisory Board Commission on Engineering and Technical Systems, National Research Council. National Academy Press, Washington DC, 1995.
[10] Brown JR, St. John NA. Fire-retardant low-temperature-cured phenolic resins and composites. Trends in Polym Sci 1996;4(12):416–420.
[11] Knopp A, Bohmer V, Pilato LA. Comprehensive polymer science, the synthesis, characterization, reactions and applications of polymers, 5. New York: Pergamon, 1989 chap. 35.
[12] Mark HF, Bikales NM, Overberger CG, Menges G, Kroschwitz JI, editors. Encyclopedia of polymer science and engineering, 11. New York: Wiley, 1988 chapter: phenolic resins.
[13] Zhang X, Looney MG, Solomon DH, Whittaker AK. Polymer 1997;38(23):5835–5848.
[14] Klett MW, Dailey TH, Jr, Allison R. New advancements in phenolic resin pultrusion. Proc. 25th Int. SAMPE Tech. Conf., October 1993.
[15] Branco CM, Ferreira JM, Fael P, Richardson MOW. A comparative study of the fatigue behaviour of GRP hand lay-up and pultruded phenolic composites. Int J Fatigue 1995;18(4):255–263.
[16] Brode GL, Chow S-W, Hale WF. Union Carbide Corp. US Patent 4,403,066. Composites Made from Liquid Phenol Formaldehyde Resins. 9/6/83.
[17] Hindersinn RR. Occidental Chemical Corp. US Patent 4,419,400. Pultruded Reinforced Phenolic Resin Products. 12/6/83.
[18] Wu H-D, Wu Y-D, Su Y-F, Ma C-CM. Pultruded fiber-reinforced polyurethane-toughened phenolic resin. II. Mechanical properties, thermal properties, and flame resistance. J Appl Polym Sci 1996;62:227–234.
[19] H. Thorning H. Phenolic matrices used for pultruded profiles. Proc. 17th Reinforced Plastics Congress, 1990, p. 284–7
[20] Walton G. Manufacturers tackle phenolic processing challenges. High Performance Composites 1998;34–38.
[21] Hshieh F, Beeson HD. Spec Tech Publ 1995;STP 1267:152–167.
[22] Hale A, Macosko CW. J Appl Polym Sci 1989;38:1253–1269.
[23] Bair HE. Proceedings of the 21st North American Thermal Analysis Society Conference. 13–16 September, 1992, Atlanta, GA. p. 60–71.
[24] Ogata M, Kinjo N, Kawata T. J Appl Polym Sci 1993;48:583–601.
[25] Biernath RW, Soane DS. In: Salamone JC, Riffle JS, editors. Contemporary topics in polymer science, 7. , 1992. pp. 103–159.
[26] Ghassemi H, Shobha HK, Sankarapandian M, Shultz A, Sensenich CL, Riffle JS, Lesko JJ, McGrath JE, Sorathia U. Void-free phenolic networks for infrastructure. Fiber composites in infrastructure, vol. 1, ICCI'98.
[27] Sankarapandian M, Shobha HK, Sensenich C, Shih P, Riffle JS, Loos AC, McGrath JE. Void-free phenolic networks. Proceedings at the 43rd International SAMPE Symposium & Exhibition. Anaheim, California, May 1998.
[28] Standard test methods for plane-strain fracture toughness and strain energy release rate of plastic materials designation: D 5045-91.
[29] Roland CM. Macromolecules 1994;27:4242–4247.
[30] Connolly M, Karasz F. Macromolecules 1995;28:1872–1881.
[31] Matsuoka S. Relaxation phenomena in polymers, New York: Hanser Publishers, 1992.
[32] Angell CA. Journal of Non-Crystalline Solids 1991;131–133:13–31.
[33] Bohmer R, Ngai KL, Angell CA, Plazek DJ. J Chem Phys 1993;99(5):4201–4209.
[34] Ngai KL, Roland CM. Macromolecules 1994;27:2454–9.